

## Wellbore integrity and corrosion of carbon steel in CO<sub>2</sub> geologic storage environments: A literature review

Yoon-Seok Choi<sup>a,\*</sup>, David Young<sup>a</sup>, Srdjan Nešić<sup>a</sup>, Linda G.S. Gray<sup>b</sup>

<sup>a</sup> Institute for Corrosion and Multiphase Technology, Department of Chemical and Biomolecular Engineering, Ohio University, Athens, OH 45701, USA

<sup>b</sup> RAE Engineering and Inspection Ltd., Edmonton, AB T6E 5M4, Canada

### ARTICLE INFO

#### Article history:

Received 24 July 2012

Received in revised form

13 December 2012

Accepted 30 December 2012

Available online 26 January 2013

#### Keywords:

Corrosion

Cement

CO<sub>2</sub>

Wellbore integrity

Carbon capture and storage

### ABSTRACT

Depleted oil and gas fields are attractive candidates for carbon capture and storage (CCS). As it contemplates the transition from CO<sub>2</sub> enhanced oil recovery (EOR) to CCS, the Weyburn–Midale CO<sub>2</sub> project is one such site. In the long-term risk assessment for Weyburn–Midale, wellbore integrity was identified as being a significant risk factor with respect to the permanence of CO<sub>2</sub> sequestration. In an optimal situation, cementing will be good for both completion and abandonment; contact of CO<sub>2</sub> with casing will be governed by cement permeability and interface effects. However, in the event of there being a poorly cemented casing-hole annular space, a more direct contact between the now “wet” injected CO<sub>2</sub> and the casing steel will be possible. Consequently, this will lead to corrosion of the steel and the potential for CO<sub>2</sub> leakage. The corrosion rate of carbon steel under high CO<sub>2</sub> pressure without protective FeCO<sub>3</sub> is very high (~20 mm/year). At certain conditions, the corrosion rate can decrease to low values (~0.2 mm/year) in long-term exposure due to the formation of a protective layer of FeCO<sub>3</sub>.

© 2013 Elsevier Ltd. All rights reserved.

### 1. Introduction

Mature oil and gas fields represent attractive candidates for the geologic storage of CO<sub>2</sub>. Such sites are well characterized, host formations are overlain by impermeable caprock that permitted hydrocarbon accumulation and operators have experience with the chemistries encountered in wellbore environments (sour character, brine, etc.).

Weyburn and Midale, depleted oil and gas fields located in southeast Saskatchewan, Canada and operated by Cenovus and Apache, respectively, are examples of such sites. Over the last decade the operators have used CO<sub>2</sub>, from Dakota Gasification's Great Plains Synfuels Plant in their enhanced oil recovery (EOR) operations to facilitate and extend production from these fields. Over 4500 wells exist at Weyburn–Midale in the area where CO<sub>2</sub> injection is occurring (Wilson and Monea, 2004). As the fields reach the end of their production lives, they may be utilized for deep geologic storage of CO<sub>2</sub>. The reservoir comprises limestone (primarily calcite (CaCO<sub>3</sub>)) and dolostone (primarily dolomite (CaMg[CO<sub>3</sub>]<sub>2</sub>)). Variable secondary amounts of quartz and metal (alumino) silicates are also present. The contained brine consists primarily of Na<sup>+</sup>, Cl<sup>-</sup>, Ca<sup>2+</sup> and SO<sub>4</sub><sup>2-</sup>. The caprock (or “primary seal”) is the Midale Evaporite unit, which is comprised primarily of anhydrite, and the ultimate seal is the Watrous Formation, a

regionally extensive aquitard comprising siliciclastics (notably, tight siltstones) with anhydritic and dolomitic cements. In spite of favorable geology, in the long-term risk assessment for the storage site, wellbore integrity was identified as being a significant risk factor with respect to the permanence of CO<sub>2</sub> sequestration.

Particular “Features, Events and Processes”, or “FEPs”, listed as being relevant to the Weyburn system that were specific to abandoned wells included the quality/integrity of annular space, unsealed boreholes, corrosion of casing, corrosion products, seal degradation and incomplete records of abandonment/sealing (Chalaturnyk et al., 2004). Therefore, prior to discussion of corrosion, consideration is given to cementing as this plays a key role in determining how dissolved CO<sub>2</sub> may contact the casing. In addition to zonal isolation, cement helps confer protection to casing against corrosive fluids.

### 2. Cementing and corrosion

In principle, casings are cemented upon completion and plugged upon abandonment to ensure isolation of the zone containing the sequestered CO<sub>2</sub>. An ideal, simplified abandoned well is depicted in Fig. 1. Note that the annular space between the casing and the rock is completely filled with cement, and the plug top is located within the caprock, thus ensuring isolation of the production zone. Therefore, if the casing is to come in contact with CO<sub>2</sub> saturated brine within the production zone/formation rock, the cement sheath itself must be infiltrated.

\* Corresponding author. Tel.: +1 740 593 9944; fax: +1 740 593 9949.

E-mail address: [choi@ohio.edu](mailto:choi@ohio.edu) (Y.-S. Choi).

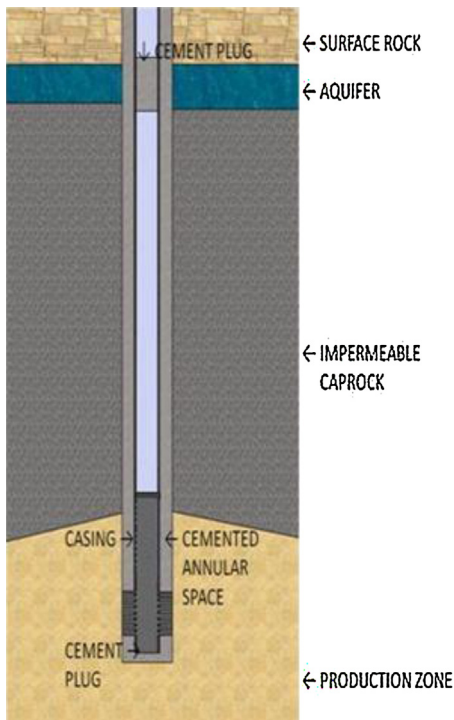


**Fig. 1.** Schematic of an ideal, simplified wellbore completion and plugging (abandonment).

### 2.1. Interfaces and microannuli

In their analysis of CO<sub>2</sub>-exposed oil-well cement from the near CO<sub>2</sub>-reservoir zone at SACROC, Carey et al. (2007) have shown that despite heavy carbonation the cement retained its low permeability, being even less permeable than the noncarbonated cement in the wellbore. They further indicated that CO<sub>2</sub> migrated along the cement/caprock and cement/casing interfaces, in the latter case speculating that CO<sub>2</sub> infiltration may have occurred due to migration up the casing wall, through casing threads or at particular points of corrosion. Consequently, the authors speculated that, "The integrity of these interfaces appears to be the most critical issue in wellbore performance for CO<sub>2</sub> sequestration". Kutchko et al. (2008) published findings consistent with Carey et al.'s SACROC study. CO<sub>2</sub> cement penetration was extrapolated to be  $1.00 \pm 0.07$  mm and  $1.68 \pm 0.24$  mm over 30 years for CO<sub>2</sub>-saturated brine and supercritical CO<sub>2</sub>, respectively, again indicating that interface effects are dominant.

Scherer et al. (2011) focused on characterizing cement from a well in the Teapot Dome oil field. The main thrust of this work was to gain information on the condition of the cement at its interfaces with both the caprock and the casing (K-55 steel) approximately 20 years after completion, but prior to any injection of CO<sub>2</sub>. Casing was recovered at both 932.7 m (3060 ft) and 1675.2 m (5496 ft), adjacent to the Second Wall Creek Sandstone and the Tensleep Sandstone dolomitic caprock, respectively. The authors reported that, "...a surprising amount of corrosion of the steel is evident. . ." for the steel recovered at 932.7 m (3060 ft), and hypothesized that this may have occurred during drilling. The figure that depicts the casing-cement interface indicates that they remain well bonded. However, orange staining of the cement in the range of 1–3 mm from the interface seems to have occurred. This may also indicate that iron oxidized during the corrosion process and produced ferrous/ferric ions that migrated toward/into the cement. This would be consistent with experimental observations made by Carey et al. (2010), showing the formation of FeCO<sub>3</sub>/Fe<sub>x</sub>CayCO<sub>3</sub> in

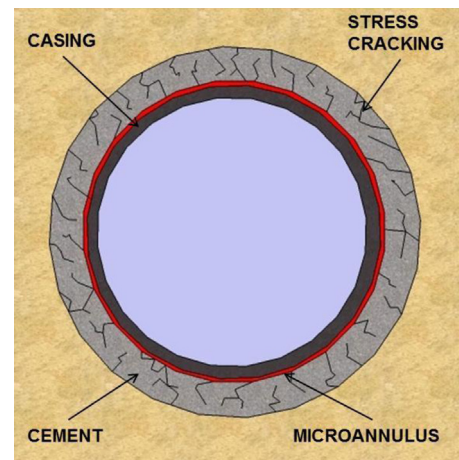


**Fig. 2.** Stress cracking of cement in the annular space.

casing–cement microannuli. In another study, Crow et al. (2010) recovered and characterized a casing–cement core from a CO<sub>2</sub> producing wellbore and noted infiltration of cement by iron corrosion product species. In their corrosion model, they expected maximum possible corrosion rates ranging from 440 to 1050 μm per year. In Scherer et al.'s (2011) work, small voids between casing and cement could also be observed. These may represent microannuli, perhaps related to thermal/pressure cycling or cement contraction, providing routes for fluid migration and promotion of corrosion. Recall that this study did not involve CO<sub>2</sub> injection. Based upon the observations made by Carey et al. (2010), it is likely that such annuli would fill with FeCO<sub>3</sub>/Fe<sub>x</sub>CayCO<sub>3</sub> and, in essence, undergo healing when exposed to high pressure CO<sub>2</sub> in the presence of water.

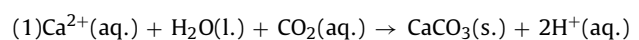
### 2.2. Cement cracking and channeling

It is likely that the above research reported by Carey et al. (2010) and Scherer et al. (2011) represents best cases. In his SPE presentation describing cementing of wellbores, Heathman (2007) discussed scenarios where integrity would be compromised. Cementing preserves zonal isolation and confers casing protection, key for optimal production. However, based upon his observations, the following sequential processes can be postulated to occur:

- Cement fluid and formation rock interaction leading to, for example, loss of shale integrity and evaporite [e.g., halite] dissolution.
- Salting of cement leading to reduced tensile strength and insufficient compressive strength.
- Cement becoming more brittle than planned and an increasing likelihood of sheath failure.
- Stress cracking.

In addition to the occurrence of microannuli at the casing–cement interface, cracks through the cement may exist. This would enable readier diffusion of species through the cement to attack the steel (see Fig. 2).

The end result would be an increased likelihood of sustained casing pressure (SCP), observed in the field in such systems, and casing corrosion. In newer cement formulations, with more elasticity, such mechanical failure is less likely to occur. In addition, considering the chemistry of Portland cements and the CO<sub>2</sub>-rich aqueous environment that will occur upon CO<sub>2</sub> injection, such cracks may also fill with CaCO<sub>3</sub> in a healing-type process:



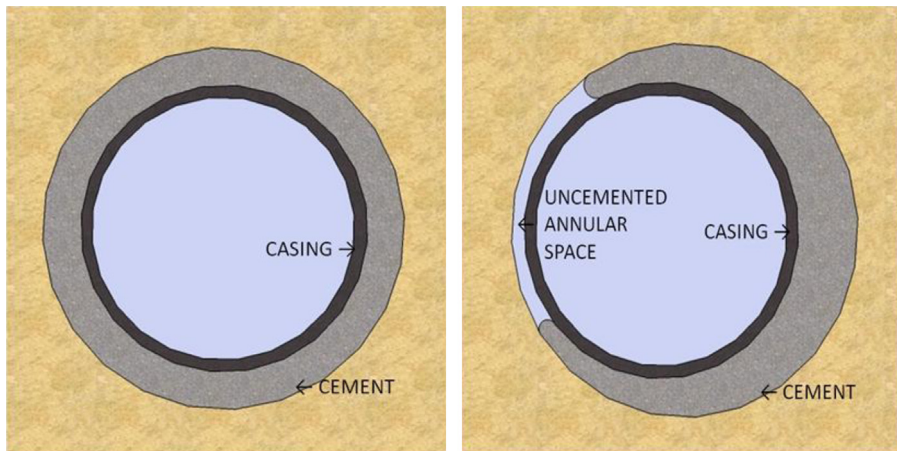


**Fig. 3.** Sections depicting ideal (left) and poor (right) mud displacements in centralized and decentralized situations.

This is similar to cement carbonation and is akin to processes that have been hypothesized to occur in microannuli during corrosion (Carey et al., 2010). Consequently, even if stress cracking does occur, there remains the possibility that cracks would fill with metal carbonates and limit diffusion of corrosive fluid to the casing. Note that in the above cases, SCP was either not discussed or was not observed. In reports submitted by researchers at Louisiana State University (LSU) to the US Department of the Interior Minerals Management Service (MMS), SCP is defined as "a pressure measurable at the casinghead of a casing annulus that rebuilds when bled down and that is not due solely to temperature fluctuations and is not a pressure that has been deliberately applied" (Bourgoyne et al., 2000; Wojtanowicz et al., 2001). This is a manifestation of gas migration into annular space. Consequently, this can indicate that there can be communication between corrosive fluids and casing, compromising the ability of cement to protect the steel. In these reports to the MMS, the incidence of SCP for surface casing strings was reported to be around 30%, the majority being in wells that were shut-in or temporarily abandoned (Bourgoyne et al., 2000). There is some debate as to whether the statistics reported by the LSU researchers correspond to actual incidences of SCP (Stress Engineering Services Inc, 2001). It is noteworthy, however, that other authors have reported completions or high levels of cement job failure that would result in casing pressure, and hence communication with potentially corrosive fluids. Tensile cracks and channels are considered to be dominant pathways for SCP (Newman et al., 2001; Watson and Bachu, 2009).

In a field case from Wamsutter, Wyoming reported by Amoco (Sauvageau, 1983), a modified technique for cementing was described that took their success rate for completion from 21% to 100%, thus eliminating the need for remedial cement squeezes. Key factors that affected cementing were reported to include insufficient annular space (poor hole condition), drilling fluid characteristics to maximize mud removal, pipe movement (reciprocation/rotation), adequate use of centralizers, preflushing of the annular space, packers and cement slurry design.

Kellingray (2007) classified annular flow into three categories:

- Percolation through unset cement.
- Influx via mud channels.
- Flow/pressure transmission through microannuli/cracks.

Further, poor mud displacement during cementing was highlighted as being a major cause of poor sheath integrity and loss of zonal isolation. Indeed, poor mud displacement would result in

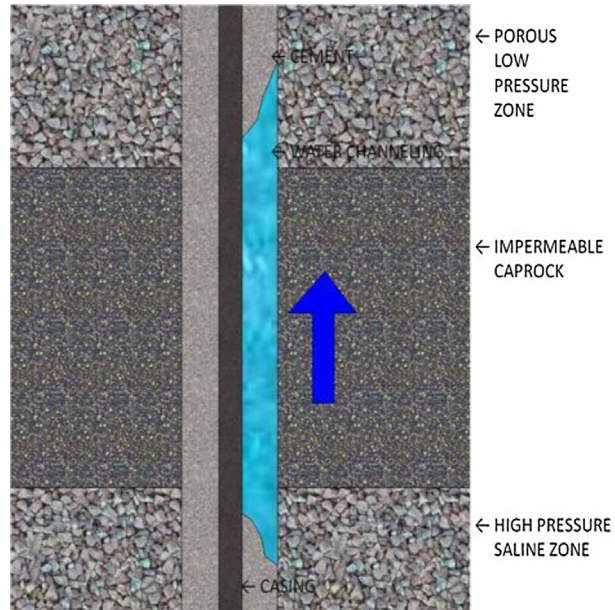


**Fig. 4.** Water channeling along a bad cement job with potential for corrosion at the casing surface.

void space occurring within the annulus as shown in Fig. 3. Gas channeling through unset cement can also lead to similar cementing problems. Such poor cementing can result in gas and water channeling along the casing that necessitates a remedial cement squeeze. If remediation is not promptly conducted, (trapped) fluid would then directly contact the unprotected casing surface, with severe corrosion and failure the likely result. Such a scenario combined with water channeling is depicted in Fig. 4; poor cementing has resulted in loss of zonal isolation, the direction of the arrow indicates flow from a high pressure zone into a lower pressure zone.

In their paper on downhole corrosion mitigation, Talabani et al. (2000) discuss the crucial role of cement presence and composition in conferring casing protection, and the use of corrosion inhibitors and cathodic protection. They go on to list four types of casing corrosion as follows:

- Erosion Corrosion – wear/abrasion occurs at the casing surface after/during drilling and insertion of casing. Salts and oxides deposit/form at the casing surface, leading to an increased likelihood of localized attack.

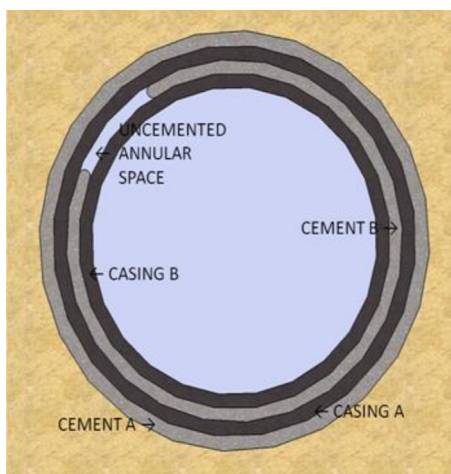


**Fig. 5.** Scenario for galvanic corrosion between two dissimilar metals across an uncemented annular space.

- Hydrogen Damage – evolved hydrogen diffuses into steel, leading to embrittlement and casing failure.
- Biological Corrosion – local colonies of bacteria change chemistry at particular regions of a casing surface; for example, sulfate reducing bacteria (SRB) forming  $H_2S$  that goes on to corrode the steel (Sherar et al., 2011).
- Galvanic Corrosion – when cement is absent and electrolyte is present between two dissimilar casings which connect electrically, one will become the anode. This leads to corrosion and leakage, see Fig. 5.

Note that such a galvanic corrosion scenario could be present when different casings are nested then poorly cemented, e.g., surface/intermediate and intermediate/production casings. In the absence of  $CO_2$ , trapped fluid would be alkaline due to the character of the cement. However, if  $CO_2$  infiltrated into this space then the pH would drop, depassivation would occur and the corrosive fluid could attack the casing. Talabani et al. (2000) went on to suggest application of coatings to inner/outer casings, removal of certain cement additives that can cause unwanted chemical reactions and addition of inhibitor to the cement in order to combat downhole corrosion.

In summary, the quality of cement jobs will play a key role in determining the degree to which casing is protected. In the best case, microannuli could inevitably be the sole pathway for fluid transport and these are likely to become filled with metal carbonates over time. Stress cracking of cement may also result in a pathway that permits corrosive fluids to attack casing, however – and especially considering cement and brine chemistry (particularly after  $CO_2$  injection) – a degree of healing may occur. In the worse case scenario, cementing is incomplete and voids exist within the annular space. Corrosion then sets in on the external surface of the casing. If this occurs between dissimilar casings, it cannot be easily remediated.

### 3. Corrosion of wellbore materials under high pressure $CO_2$ conditions

The impact of  $CO_2$  corrosion on low alloy steels has been studied extensively at pressures relevant for oil and gas transport (up to 1 MPa  $CO_2$ ). Many researchers have theorized the mechanisms of  $CO_2$  corrosion of steels and have attempted to predict the corrosion rate (Nesic, 2007). However little work has been carried out on high pressure wet  $CO_2$  corrosion, especially over 7.38 MPa which is the supercritical pressure of  $CO_2$ .

Early study in high  $pCO_2$  corrosion was related to the  $CO_2$  enhanced oil recovery (EOR) process. Kapusta and Canter (1994) summarized Shell's experience with corrosion and corrosion control at the Little Creek Field (MS)  $CO_2$  enhanced oil recovery project. The first producing wells were turned on in 1986 with 24.1 MPa and 115 °C of bottom hole pressure and temperature. The produced water had very high TDS (total dissolved solids), and a relatively high  $CaCO_3$  scaling tendency with 96,700 mg/L  $Cl^-$ , 79 mg/L  $SO_4^{2-}$ , 473 mg/L  $HCO_3^-$ , 15200 mg/L  $Ca^{2+}$ , 243 mg/L  $Mg^{2+}$  and 14 mg/L  $Ba^{2+}$ , as well as  $Na^+$ . Most wells were completed using internally plastic coated (baked phenolic coating) low alloy steel tubing (N-80 in the upper 1/3 of the well, down to about 823 m, and J-55 in the lower section), and a 13Cr (AISI 410) stainless steel wellhead. This work illustrated some of the problems encountered during the implementation of a corrosion control program for high  $CO_2$  wells:

- The selective lack of protection of N-80 grade steel.
- The importance of using the correct metallurgy for inhibitor testing.
- The poor correlation of surface monitoring techniques with downhole corrosion rates.
- Emulsion problems caused by inhibition.
- The importance of complementing lab tests with field trials.

According to visual examination of production tubing from the field (pressure: 5.92–12.2 MPa; temperature: 40–44 °C), corrosion rates were about 6.35 mm/year on the N-80 tubing and 0.13 mm/year on J-55 tubing after 10 months of production. In addition, based on the chemical composition of samples, it was known that severely corroded steel contained more than 0.6% Cr; less corroded steel contained less than 0.3% Cr. They also conducted laboratory tests in static autoclaves and in the flow-through system (test conditions are not shown in the article). Tests in a static autoclave showed that N-80 (7.6 mm/year) had a lower average corrosion rate than J-55 (12.7 mm/year) for one day-exposure. Results from a flow-through system (Once Through Corrosion Test Facility; OTCTF) also showed that N-80 (38.1 mm/year) had a lower corrosion rate than J-55 (50.8 mm/year) under uninhibited conditions. However, N-80 was not protected using field inhibitors at a 300 ppm concentration showing corrosion rates of 25.4 mm/year for N-80, but 2 mm/year for J-55.

Russick et al. (1996) conducted a study of the corrosive effects of supercritical  $CO_2$  on C1018 carbon steel. Corrosion testing (weight loss measurement) of metals was performed in pure supercritical  $CO_2$  and in water-saturated supercritical  $CO_2$ . No corrosion was observed on the sample in dry supercritical  $CO_2$  exposure at 24.1 MPa and 50 °C for 24 h. Water-saturated supercritical  $CO_2$  did, however, cause visually obvious signs of corrosion at the same pressure and temperature. However, the corrosion rate values determined as weight changes were too small to be measured accurately.

Propp et al. (1996) performed ER (electrical resistance) measurements to monitor the corrosion of iron in pure supercritical  $CO_2$ . They used a closed, small volume, thermal loop for the corrosion study. The sample was exposed to supercritical  $CO_2$  at 8.7–12.2 MPa and 162–183 °C for 5000 h. Despite the fluid being pure supercritical  $CO_2$ , corrosion rates ranging from 0.0025 to 0.01 mm/year were obtained due to the high temperature.

Cui et al. (2004, 2006) investigated the corrosion property of three pipeline steels (J-55, N-80, P-110) in static simulated produced water (SPW:  $CaCl_2$  15,000 mg/L,  $NaHCO_3$  1100 mg/L, pH range 4–6.) saturated with supercritical  $CO_2$  using weight loss measurements. They analyzed the chemical composition and structure of the corroded surface using surface analytical techniques (SEM, XRD and XPS). The sample was exposed to the solution which is saturated with supercritical  $CO_2$ . Supercritical  $CO_2$  was achieved by

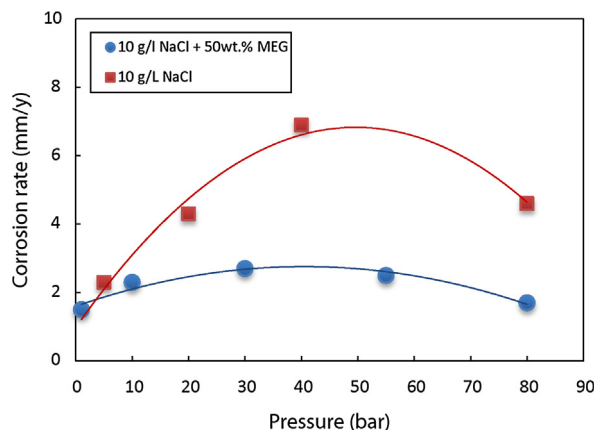


**Fig. 6.** Corrosion rates of the samples in  $\text{CO}_2$ -saturated water with/without 50 wt.% MEG solution at 50 °C as a function of pressure.

Data from Seiersten and Kongshaug (2005).

compressing the system to the required pressure of 8.274 MPa and heating to 60, 90, 120 and 150 °C. The results showed that the corrosion rates sharply decreased as the temperature increased from 60 to 90 °C, from approximately 2 mm/year to 1 mm/year for J-55 steel. Corrosion rates halved again from 90 to 150 °C. The authors claimed that the decrease of the corrosion rates resulted from the passivation of the surface by corrosion product formation on the steels associated with  $\text{CO}_2$  corrosion. The surface film on the corroded surface was mainly composed of  $\text{FeCO}_3$  and  $\alpha\text{-FeOOH}$ . The scale that formed at a high temperature was more compact and continuous, and hence more protective, than that formed at low temperature. They also claimed that the decrease of the solubility of  $\text{CO}_2$  in water with increasing temperature resulted in a lower concentration of carbonic acid in the system.

Seiersten and Kongshaug (2005) determined the corrosion rate of X65 carbon steel as function of  $\text{CO}_2$  pressures up to 8.0 MPa and temperatures up to 50 °C. They used an autoclave with a circulation pump. The samples were immersed in both water-saturated  $\text{CO}_2$  and  $\text{CO}_2$ -saturated water phases. The corrosion rate was measured by the linear polarization resistance (LPR) technique for samples in the  $\text{CO}_2$ -saturated water phase. The results showed that the corrosion samples mounted in the  $\text{CO}_2$  phase at the top of the autoclave did not show any sign of corrosion attack. However, supercritical  $\text{CO}_2$  with water content above saturation is corrosive when water precipitates so they tested in  $\text{CO}_2$ -saturated water to evaluate the corrosive potential of free water. Fig. 6 shows the relationship between the corrosion rates and pressures in the  $\text{CO}_2$ -saturated water phase at 50 °C with/without monoethyleneglycol (MEG). As shown in Fig. 6, the corrosion rate reached a maximum of 6.9 mm/year at 4.0 MPa and then decreased to 4.6 mm/year at 8.0 MPa, the supercritical  $\text{CO}_2$  condition. A similar behavior with respect to the influence of increased pressure reducing corrosion rates was observed in systems containing 50 wt.% MEG. Here the corrosion rate had a maximum of 2.7 mm/year at 3.0 MPa, and then decreased to 1.7 mm/year at 8.0 MPa.

Lin et al. (2006) investigated the effect of  $\text{CO}_2$  partial pressure (1.38–10.34 MPa) on the microstructure of the scales and the corrosion rates for three pipeline steels (J-55, N-80, P-110) in  $\text{CO}_2$ -saturated solution at 90 °C using scanning electron microscopy (SEM) and weight loss measurements. The results showed that the corrosion product layer thickness reached its maximum value at 6.89 MPa and then decreased with increasing  $\text{CO}_2$  pressure. They claimed that this was related to the special property of supercritical  $\text{CO}_2$  which possesses an inhibiting function in the  $\text{CO}_2$  corrosion process. Above the critical pressure,  $\text{CO}_3^{2-}$  concentration (the product of the second ionization from  $\text{H}_2\text{CO}_3$ ) at the beginning of the

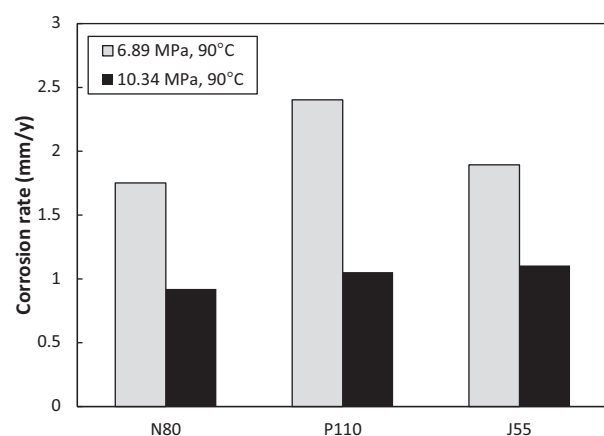


**Fig. 7.** Corrosion rates of the samples at subcritical and supercritical  $\text{CO}_2$  conditions.

Data from Lin et al. (2006).

corrosion process was higher than that below the critical pressure due to the high solubility of  $\text{CO}_2$  in water. Consequently, more crystal nuclei formed and the eventual crystal grain size was finer. The scale that formed on the steel was denser and conferred superior surface coverage, which results in a decrease in the layer thickness.

Fig. 7 shows the corrosion rates of the samples at 6.89 MPa, 90 °C (subcritical  $\text{CO}_2$ ) and 10.34 MPa, 90 °C (supercritical  $\text{CO}_2$ ) measured by weight loss tests. The corrosion rates measured at subcritical conditions showed higher values (1.7–2.4 mm/year) than measured at supercritical conditions (0.9–1.1 mm/year), which corresponded to the above presumption.

Recently, Choi and Nesic (2011) conducted a series of high  $\text{CO}_2$  pressure corrosion tests at different pressures (4.0–8.0 MPa) and temperatures (25–70 °C) related to the corrosion in  $\text{CO}_2$  transport pipelines. The corrosion rates of carbon steel in  $\text{CO}_2$ -saturated water were very high (~20 mm/year), indicating a high risk associated with corrosion when high pressure anhydrous  $\text{CO}_2$  interacts with water, a situation encountered, for example, for casings in a saline aquifer.

In addition, Choi et al. (2010) performed corrosion tests to evaluate the effect of  $\text{O}_2$  on high pressure  $\text{CO}_2$  corrosion. Fig. 8 shows the corrosion rates of X65 mild steel in a  $\text{CO}_2$ -saturated water phase with and without  $\text{O}_2$  as a function of the test period at 50 °C. As shown in Fig. 8, over a long period of time, the addition of  $\text{O}_2$  in the

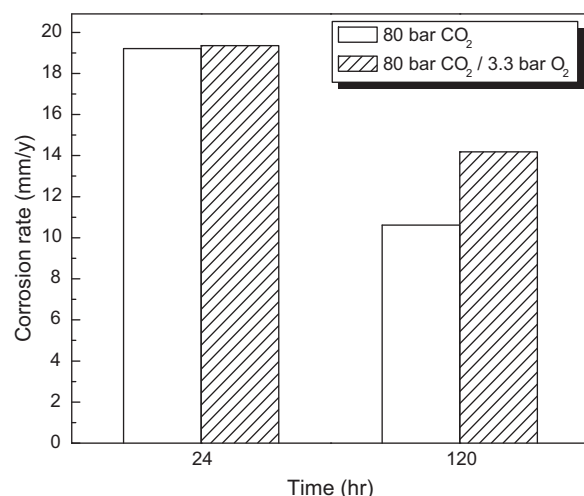


**Fig. 8.** Effects of oxygen and exposure time on the corrosion rates of mild steel in water-rich phase.

Data from Choi et al. (2010).

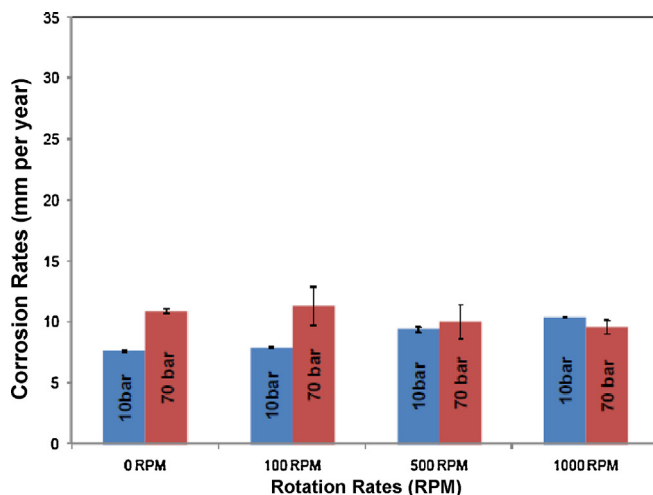


**Fig. 9.** Comparison of corrosion rate from LPR measurements between  $p\text{CO}_2 = 1 \text{ MPa}$  and  $7 \text{ MPa}$  at  $25^\circ\text{C}$  and pH 3.

Data from Mohammed Nor et al. (2011).

system increased the corrosion rate of carbon steel by inhibiting the formation of protective  $\text{FeCO}_3$  on the steel surface.

Loizzo et al. (2009) conducted laboratory experiments to characterize possible steel degradation mechanisms under  $\text{CO}_2$  storage conditions. They exposed N-80 and J-55 casing steels in an electrolyte with similar composition as the formation water of the well, under pressurized  $\text{CO}_2$  conditions ( $8.0 \text{ MPa CO}_2$ ,  $45^\circ\text{C}$ ). The results showed that uniform corrosion is the most likely degradation mechanism in steel; the formation of a protective ferrous oxide layer was also shown to slow corrosion rates (corrosion rates were not reported in the article). The experiments also showed that electrochemical methods, especially electrochemical impedance spectroscopy (EIS) and linear polarization resistance (LPR) measurements, could become useful for monitoring *in situ* corrosion of well materials in underground  $\text{CO}_2$  storage conditions.

Mohammed Nor et al. (2011) investigated the effect of flow on the corrosion of carbon steel in high  $p\text{CO}_2$  conditions using a high pressure and high temperature (HPHT) autoclave equipped with a rotating cylinder electrode (RCE) assembly. API X65 carbon steel was exposed to 1 wt.% NaCl at liquid velocities of 0, 0.1, 0.5 and 1.0 m/s (0, 100, 500 and 1000 rpm). Fig. 9 shows the comparison of the corrosion rates obtained from LPR measurements between  $p\text{CO}_2$  of 1.0 MPa and 7.0 MPa at  $25^\circ\text{C}$  and pH 3. It can be seen that the corrosion rate has only a slight sensitivity to the change in velocity at high  $p\text{CO}_2$ . They claimed that the increase in  $\text{CO}_2$  partial pressure reduced the flow-sensitivity of the  $\text{CO}_2$  corrosion rate due to the increase in carbonic acid ( $\text{H}_2\text{CO}_3$ ) concentration.

Zhang et al. (2011) performed rotated cage corrosion experiments (4 m/s) in a  $\text{CO}_2$  saturated water phase in order to investigate the performance of corrosion inhibitors in supercritical  $\text{CO}_2$  systems. The materials tested included two carbon steels: a downhole tubing steel type 38Mn6/C75 (Quenched and Tempered martensitic-bainitic microstructure) and a pipeline steel type X65 (ferritic-pearlitic microstructure), and three Cr-containing steels [(i) X20Cr 13 (1.4021, UNS 42000; martensitic microstructure), (ii) X2CrNiMoN 22-5-3 (1.4462, UNS S31803, duplex microstructure) and (iii) X1NiCrMCu 25-20-5 (1.4539, alloy 904L, UNS N 08904; austenitic microstructure)]. The supercritical conditions were achieved by metering 450 g liquid  $\text{CO}_2$  into 1000 g  $\text{H}_2\text{O}$  in the autoclave and subsequently heating to  $50^\circ\text{C}/9.5 \text{ MPa}$ ,  $80^\circ\text{C}/13.5 \text{ MPa}$ ,  $110^\circ\text{C}/17.0 \text{ MPa}$  and  $130^\circ\text{C}/21.5 \text{ MPa}$ , respectively.

The corrosion rates ranged from 5 to 14 mm/year in the case of carbon steels with slightly higher rates for the X65 steel. Maximum

corrosion rates were encountered at  $80^\circ\text{C}$ . The inhibitors tested included two types of oleic acid based imidazolines, hexadecenyl succinic anhydride, and hexadecyltrimethylammonium (HTA) bromide. The imidazoline 18-OH showed the lowest efficiency for carbon steel and the best performance was found for the quaternary ammonium compound. In addition, it can be seen that all inhibitors tested are effective not only for carbon steels but also for the Cr and CrNi steels and showed the same ranking of the inhibitor efficiencies.

It is important to note that considerable pitting was observed on the low alloy steels in all experiments without and with corrosion inhibitors (Table 1). The lowest pit intensity was found with HTA bromide. However, even with this inhibitor the pit depth still reached about 30  $\mu\text{m}$  after 96 h exposure.

Han et al. (2011a) conducted corrosion experiments to assess the corrosion risk at the cement-steel interface under *in situ* wellbore conditions. They focused on the mass transfer effect by substituting cement with inert epoxy which created a gap (20 or 100  $\mu\text{m}$ ) with J-55 steel in order to simulate the cement-steel interface. The tests were conducted in an autoclave with 1 wt.% NaCl at 10 MPa  $\text{CO}_2$  and  $50^\circ\text{C}$  for 7 days. For open surface condition (without epoxy), the initial corrosion rate was about 10 mm/year and it decreased after a few hours of exposure due to the formation of  $\text{FeCO}_3$  on the steel surface. After 7 days, the corrosion rate was about 0.3 mm/year. For the interface gap sample (100  $\mu\text{m}$ ), the corrosion rate increased from about 0.1 to 1 mm/year over the 7 days of the test. They claimed that the 100  $\mu\text{m}$  interface gap restricts maximum corrosion rates in this system to 1–2 mm/year and the  $\text{FeCO}_3$  film limits corrosion rates to 0.2–0.4 mm/year. In addition, they found that the interface gap only affected initial corrosion rates while long-term corrosion rates were limited by diffusion through the corrosion scale rather than by diffusion along the interface gap.

Han et al. (2012) extended their study to a degradation of cement-steel composites in supercritical  $\text{CO}_2$ -saturated brines. They found that corrosion rate dramatically increased when the cement was partially carbonated and the pre-formed passive film was damaged. Then it decreased to an initial level due to the formation of scales containing calcium/iron carbonates. It is interesting to note that no corrosion protection was provided by fully carbonated cement; instead it showed the most severe corrosion rate.

Since  $\text{CO}_2$  corrosion is an electrochemical phenomenon, it is not surprising that a number of researchers started out with mathematical modeling of corrosion by describing the electrochemical processes occurring at the metal surface. However, these models only cover low pressure ranges and they over-predict the corrosion rate (usually an order of magnitude too high) at high  $p\text{CO}_2$  conditions. This indicates that the corrosion mechanism at high pressure (liquid and supercritical  $\text{CO}_2$ ) is different from the classic theory which has been applied for low to moderate  $\text{CO}_2$  pressure. To date there have been very few mechanistic studies of uniform and localized corrosion under high  $p\text{CO}_2$  conditions (Han et al., 2011b).

#### 4. Implications for Weyburn–Midale and other injection sites

Many of the wells at Weyburn–Midale are approaching 60 years old and will have been completed with a variety of methods using different casing steels and various grades of cement. Field data from Weyburn indicates dominant use of J-55, carbon steel, casing with some use of H-40 and minor application of other alloys. Furthermore, various well abandonment procedures will have been applied, particularly as practices evolved over time (e.g., Government of Saskatchewan, 1985; Railroad Commission of Texas, 1995, 2000). A commonly used abandonment at Weyburn is depicted in Fig. 1. Note that the casing is completely isolated

**Table 1**

Effect of temperature and type of inhibitor on the pit density and maximum pit depth for carbon steels in the system 450 g CO<sub>2</sub>/1000 g H<sub>2</sub>O.

Steel type	50 °C		80 °C		110 °C		130 °C	
	Pit D (pits/mm <sup>2</sup> ) <sup>a</sup>	Max. D (μm) <sup>a</sup>	Pit D (pits/mm <sup>2</sup> )	Max. D (μm)	Pit D (pits/mm <sup>2</sup> )	Max. D (μm)	Pit D (pits/mm <sup>2</sup> )	Max. D (μm)
No inhibitor								
38Mn6/C75	0.095	38	0.194	85	0.155	76	0.116	47
X65	0.128	46	0.287	95	0.242	88	0.135	72
100 ppm Imidazoline 18-OH								
38Mn6/C75	n.e. <sup>a</sup>	n.e.	0.179	72	n.e.	n.e.	n.e.	n.e.
X65	n.e.	n.e.	0.266	84	n.e.	n.e.	n.e.	n.e.
100 ppm Imidazoline 18-NH								
38Mn6/C75	0.064	30	0.1155	56	0.09	53	0.076	39
X65	0.095	36	0.192	66	0.145	62	0.113	49
100 ppm Hexadecenyl succinic anhydride (HSA)								
38Mn6/C75	0.056	31	0.105	44	0.084	40	0.068	37
X65	0.084	36	0.138	48	0.112	44	0.092	41
100 ppm Hexadecyl-trimethylammonium bromide (HTA bromide)								
38Mn6/C75	0.048	29	0.083	37	0.069	34	0.054	33
X65	0.076	33	0.114	44	0.092	38	0.077	34

Data from Zhang et al. (2011).

<sup>a</sup> Pit D = pit density; Max. D = maximum pit depth; n.e. = no experiment because of poor inhibitor efficiency.

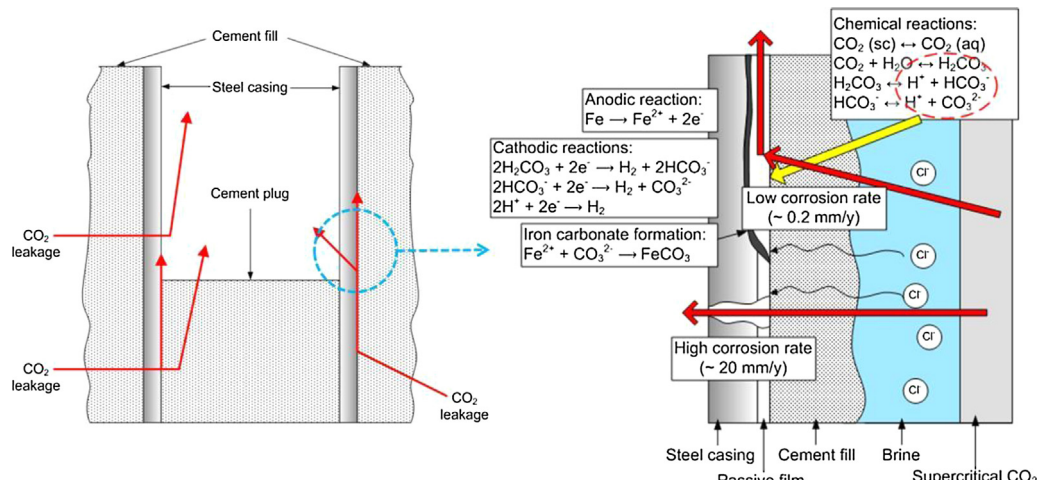


Fig. 10. Loss of wellbore integrity due to corrosion and CO<sub>2</sub> leakage.

from the formation rock, both by cement in the annular space and by cement squeezed into the perforations in the production zone. A cement retainer is also placed above the perforations, usually within 5 m of the perforations.

As discussed above, however, should there be incomplete cementing in the annular space or cement degradation, then casing will become directly exposed to fluids. This will likely correspond to reservoir brine, containing dissolved corrosive species such as CO<sub>2</sub>, H<sub>2</sub>S and organic acids. Consequently, the steel casing, with no protection conferred by a cement sheath, will undergo severe corrosion. In the presence of wet, high pressure CO<sub>2</sub>, this could occur at corrosion rates approaching 20 mm/year. A schematic depicting such a situation is shown in Fig. 10. Note that communication between fluid and steel may occur via microannuli along the cement-casing interface, through stress cracks within the cement or through uncemented regions within the annular space. In wet, high pressure CO<sub>2</sub> the steel surface would de-passivate, resulting in corrosion along and into the casing. If this occurred above the plug, or if the plug itself has failed, then the integrity of the wellbore would be lost.

## 5. Conclusions

A wide range of wellbore completions and abandonments will be encountered in the field. Of key importance to corrosion, and

hence wellbore integrity, will be the nature and quality of cementing in the annular space. Poor cementing will result in little protection of casing, and the likelihood of corrosion will dramatically increase. Consequently, thorough evaluation of cement jobs is an essential part of corrosion prediction and protection, as well as assurance of wellbore integrity.

Based on the reviewed literature, it is known that the corrosion rate of carbon steel under high CO<sub>2</sub> pressure without protective FeCO<sub>3</sub> is very high (~20 mm/year). At certain conditions, the corrosion rate can decrease to low values (~0.2 mm/year) in long-term exposure due to the formation of a protective film of FeCO<sub>3</sub>. However, according to laboratory and field experiences, there is a possibility of localized corrosion (mesa-type) for carbon steel even with corrosion inhibitors which could dramatically reduce the lifetime of casing steel.

## Acknowledgement

The authors are grateful to the Petroleum Technology Research Centre for providing financial support for this project.

## References

- Bourgoyne, A.T., Scott, S.L., Manowski, W., 2000. A Review of Sustained Casing Pressure Occurring on the OCS. LSU, Baton Rouge, LA.

- Carey, J.W., Wigand, M., Chipera, S.J., WoldeGabriel, G., Pawar, R., Lichtner, P.C., Wehner, S.C., Raines, M.A., Guthrie Jr., G.D., 2007. Analysis and performance of oil well cement with 30 years of CO<sub>2</sub> exposure from the SACROC Unit, West Texas, USA. *International Journal of Greenhouse Gas Control* 1, 75–85.
- Carey, J.W., Svec, R., Grigg, R., Zhang, J., Crow, W., 2010. Experimental investigation of wellbore integrity and CO<sub>2</sub>-brine flow along the casing-cement microannulus. *International Journal of Greenhouse Gas Control* 4, 272–282.
- Chalaturnyk, R., Zhou, W., Stenhouse, M., Sheppard, M., Walton, F., 2004. Theme 4: long-term risk assessment of the storage site, IEA GHG Weyburn CO<sub>2</sub> monitoring and storage project summary report 2000–2004. In: 7th International Conference on Greenhouse Gas Control Technologies.
- Choi, Y.S., Nesic, S., Young, D., 2010. Effect of impurities on the corrosion behavior of CO<sub>2</sub> transmission pipeline steel in supercritical CO<sub>2</sub>-water environments. *Environmental Science and Technology* 44, 9233–9238.
- Choi, Y.S., Nesic, S., 2011. Determining the corrosive potential of CO<sub>2</sub> transport pipeline in high pCO<sub>2</sub>-water environments. *International Journal of Greenhouse Gas Control* 5, 788–797.
- Crow, W., Carey, J.W., Gasda, S., Williams, D.B., Celia, M., 2010. Wellbore integrity analysis of a natural CO<sub>2</sub> producer. *International Journal of Greenhouse Gas Control* 4, 186–197.
- Cui, Z.D., Wu, S.L., Li, C.F., Zhu, S.L., Yang, X.J., 2004. Corrosion behavior of oil tube steels under conditions of multiphase flow saturated with super-critical carbon dioxide. *Materials Letters* 58, 1035–1040.
- Cui, Z.D., Wu, S.L., Zhu, S.L., Yang, X.J., 2006. Study on corrosion property of pipelines in simulated produced water saturated with supercritical CO<sub>2</sub>. *Applied Surface Science* 252, 2368–2374.
- Government of Saskatchewan, 1985. The Oil and Gas Conservation Regulations. Saskatchewan, Regina.
- Han, J., Carey, J.W., Zhang, J., 2011a. Effect of Debonded Interfaces on Corrosion of Mild Steel Composites in Supercritical CO<sub>2</sub>-Saturated Brines, CORROSION/2011, NACE, Houston, TX, Paper No. 11376.
- Han, J., Carey, J.W., Zhang, J., 2011b. A coupled electrochemical-geochemical model of corrosion for mild steel in high-pressure CO<sub>2</sub>-saline environments. *International Journal of Greenhouse Gas Control* 5, 777–787.
- Han, J., Carey, J.W., Zhang, J., 2012. Degradation of Cement–Steel Composite at Bonded Steel–Cement Interfaces in Supercritical CO<sub>2</sub> Saturated Brines Simulating Wellbore Systems, CORROSION/2012, NACE, Houston, TX, Paper No. 0001075.
- Heathman, J., 2007. Critical Application Cementing – Redefining the Issues. Society of Petroleum Engineers Distinguished Lecturer Series, Richardson, TX, USA.
- Kapusta, S.D., Canter, S.C., 1994. Corrosion Control in CO<sub>2</sub> Enhanced Oil Recovery, CORROSION/94, NACE, Houston, TX, Paper No. 10.
- Kellingray, D., 2007. Cementing – Planning for Success to Ensure Isolation for the Life of the Well. Society of Petroleum Engineers Distinguished Lecturer Series, Richardson, TX, USA.
- Kutchko, B.G., Strazisar, B.R., Lowry, G.V., Dzombak, D.A., Thaulow, N., 2008. Rate of CO<sub>2</sub> attack on hydrated class H well cement under geologic sequestration conditions. *Environmental Science and Technology* 42, 6237–6242.
- Lin, G., Zheng, M., Bai, Z., Zhao, X., 2006. Effect of temperature and pressure on the morphology of carbon dioxide corrosion scales. *Corrosion* 62, 501–507.
- Loizzo, M., Bressers, P., Benedictus, T., Le Guen, Y., Poupart, O., 2009. Assessing CO<sub>2</sub> interaction with cement and steel over a two-year injection period: current state and future risks for the MovECBM project in Poland. *Energy Procedia* 1, 3579–3586.
- Mohammed Nor, A., Suhor, M.F., Mohamed, M.F., Singer, M., Nesic, S., 2011. Corrosion of Carbon Steel in High CO<sub>2</sub> Environment: Flow Effect, CORROSION/2011, NACE, Houston, TX, Paper No. 11242.
- Nesic, S., 2007. Key issues related to modelling of internal corrosion of oil and gas pipelines – a review. *Corrosion Science* 49, 4308–4338.
- Newman, K., Wojtanowicz, A., Gahan, B., 2001. Cement pulsation improves gas well cementing. *World Oil*, 89–94.
- Propp, W.A., Carleson, T.E., Wai, C.M., Taylor, P.R., Daehling, K.W., Huang, S., Abdellatif, M., 1996. Corrosion in Supercritical Fluids, US Department of Energy Report, DE96014006, Washington DC.
- Railroad Commission of Texas, 1995. Well Completion and Plugging Procedures Reference Manual. Oil and Gas Division, Austin, TX.
- Railroad Commission of Texas, 2000. Well Plugging Primer. 2000. Well Plugging Section. Oil and Gas Division, Austin, TX.
- Russick, E.M., Poulter, G.A., Adkins, C.L.J., Sorenson, N.R., 1996. Corrosive effects of supercritical carbon dioxide and cosolvents on metals. *Journal of Supercritical Fluids* 9, 43–50.
- Sauvageau, K., 1983. A proven technique for liner cementing in the Greater Green River Basin, Wyoming. In: Proceedings SPE/IADC Drilling Conference, pp. 471–473.
- Scherer, G.W., Kutchko, B., Thaulow, N., Duguid, A., Mook, B., 2011. Characterization of cement from a well at Teapot Dome Oil Field: implications for geologic sequestration. *International Journal of Greenhouse Gas Control* 5, 115–124.
- Seiersten, M., Kongshaug, K.O., 2005. Materials Selection for Capture, Compression, Transport and Injection of CO<sub>2</sub>, Carbon Dioxide Capture for Storage in Deep Geologic Formations, vol. 2. Elsevier, Kidlington, Oxford, UK, p. 937.
- Sherar, B., Power, I., Keech, P., Mitlin, S., Southam, G., Shoesmith, D., 2011. Characterizing the effect of carbon steel exposure in sulfide containing solutions to microbially induced corrosion. *Corrosion Science* 53, 955–960.
- Stress Engineering Services Inc., 2001. Best Practices for Prevention and Management of Sustained Casing Pressure. Stress Engineering Services, Inc, Houston, TX.
- Talabani, S., Atlas, B., Al-Khatiri, M., Islam, M., 2000. An alternate approach to down-hole corrosion mitigation. *Journal of Petroleum Science and Engineering* 26, 41–48.
- Watson, T.L., Bachu, S., 2009. Evaluation of the potential for gas and CO<sub>2</sub> leakage along wellbores. *SPE Drilling & Completion* 24, 115–126.
- Wilson, M., Monea, M., 2004. IEA GHG Weyburn CO<sub>2</sub> monitoring and storage project summary report 2000–2004. In: 7th International Conference on Greenhouse Gas Control Technologies.
- Wojtanowicz, A.K., Nishikawa, S., Rong, R., 2001. Diagnosis and Remediation of Sustained Casing Pressure in Wells. LSU, Baton Rouge, LA.
- Zhang, Y., Gao, K., Schmitt, G., 2011. Inhibition of Steel Corrosion Under Aqueous Supercritical CO<sub>2</sub> Conditions, CORROSION/2011, NACE, Houston, TX, Paper No. 11379.